Single-transverse-mode output from a fiber laser based on multimode interference

X. Zhu,* A. Schülzgen, H. Li, L. Li, Q. Wang, S. Suzuki, V. L. Temyanko, J. V. Moloney, and N. Peyghambarian

College of Optical Sciences, University of Arizona, 1630 East University Boulevard, Tucson, Arizona 85721, USA
**Corresponding author: xszhu@email.arizona.edu*

Received January 7, 2008; revised March 12, 2008; accepted March 14, 2008; posted March 20, 2008 (Doc. ID 91371); published April 22, 2008

An alternative original approach to achieve single-transverse-mode laser emissions from multimode (MM) active fibers is demonstrated. The fiber cavity is constructed by simply splicing a conventional passive single-mode fiber (SMF-28) onto a few centimeters-long active MM fiber section whose length is precisely controlled. Owing to the self-imaging property of multimode interference (MMI) in the MM fiber, diffraction-limited laser output is obtained from the end of the SMF-28, and the MMI fiber laser is nearly as efficient as the corresponding MM fiber laser. Moreover, because of the spectral filtering effect during in-phase MMI, the bandwidth of the MMI fiber laser is below 0.5 nm. © 2008 Optical Society of America

OCIS codes: 060.2320, 060.3510, 140.3500, 140.3510.

Power levels of single-mode (SM) optical fiber lasers have been significantly elevated after the design of doubly clad fibers was introduced to enable cladding-pumping with low-brightness semiconductor laser diode arrays. However, as the output power surpasses certain levels, nonlinear effects, thermo-optic effects, output power saturation, and optical damage inevitably arise as constraints of further power scaling of conventional single-mode fiber (SMF) lasers. An increase in the mode field area of the active SMF is an effective solution to overcome the constraints described herein. Large-mode-area SMFs can be realized either by precise control of the index step between the core and cladding or use of the microstructured fiber. To date, for instance, 2 kW 1 μm silica-hosted, 10 W 2.78 μm ZBLAN-hosted [1], and 2 W 1.53 μm single-frequency phosphate-hosted [2] SMF lasers have been demonstrated using large-mode-area SMFs.

However, further significantly increasing the diffraction-limited output from these record-breaking fiber lasers is technically restrained. Utilizing active multimode (MM) fibers is an alternative approach to increase mode volume and boost power levels of SM emission. Diffraction-limited outputs from active MM fibers can be obtained by introducing a discrimination mechanism between the various fiber modes that suppresses the transverse modes other than the fundamental mode. Fundamental-mode surviving mechanisms can be realized, e.g., by adjusting the fiber index and doping distribution [3,4], introducing special cavity configurations [5,6], coiling the MM fiber [7], or designing helical-core [8] or leakage channel fibers [9]. Utilizing beam cleanup effects based on stimulated Raman scattering [10] and stimulated Brillouin scattering [11] have also been proposed to obtain diffraction-limited emissions from MM fiber lasers.

In this Letter, a new concept to achieve single-transverse-mode output from an active MM fiber is proposed and demonstrated. By utilizing the self-imaging property of multimode interference (MMI) in the MM fiber, diffraction-limited output can be obtained from a highly efficient diode-pumped MMI fiber laser consisting of a short Er/Yb codoped phosphate MM fiber and a conventional SMF (SMF-28). Compared with previous techniques, MMI fiber lasers are easy to construct and do not need any specially designed fibers. In addition, because of the intrinsic properties of MMI, a narrow linewidth output can be obtained from MMI fibers without using any spectral filter.

MMI has already been widely utilized in the design and fabrication of low-loss waveguide couplers with applications such as switches, modulators, coherent receivers, and ring lasers [12]. In recent years, there has been growing interest in the application of MMI effects in fiber optics. Several groups have demonstrated MMI effects in MM fibers and fabricated MMI fiber devices for different applications, such as a multiwavelength fiber laser [13], wavelength tunable laser [14], all-fiber bandpass filter [15], wavelength tunable fiber lens [16], all-fiber refractometer sensor [17], fiber-optic displacement sensor [18], and high-temperature sensor [19].

According to the self-imaging principle of MMI effects, an input field profile is always reproduced at periodic intervals along the propagation direction of the MM waveguide. Consequently, for a diffraction-limited input field incident on the input facet of an MM fiber, MMI effects result in periodic longitudinal locations within the fiber where the source field is recovered. Therefore, when an MM fiber is sandwiched between two SMFs and the length of the MM fiber is precisely controlled to enable self-imaging of the input field, high transmission of a diffraction-limited field through an MM fiber can be obtained [15,20]. A typical transmission spectrum of a 20 cm phosphate MM fiber with a core diameter of 25 μm spliced with two SMF-28 fibers is shown in Fig. 1. For certain wavelengths, self-imaging of the input diffraction-limited field occurs and the propagation loss is only ~1 dB. Therefore, an MMI fiber laser cavity with low round-trip loss can be constructed by splicing an SMF onto a rare-earth-doped MM fiber. Because the transmission spectrum of an MMI fiber laser cavity

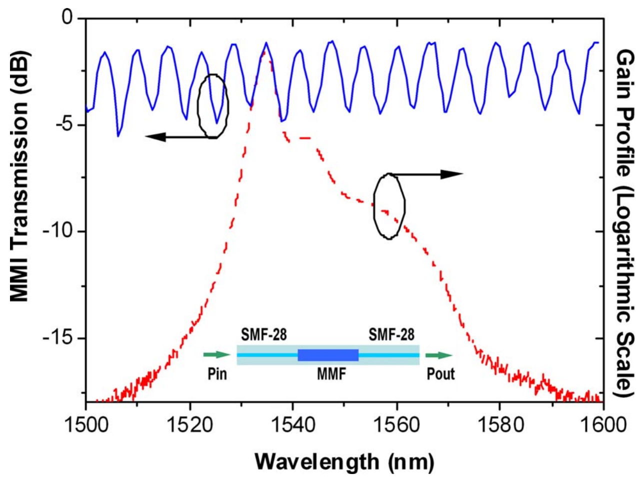

Fig. 1. (Color online) Gain profile of a heavily Er/Yb codoped phosphate fiber (dashed curve) and the transmission spectrum of an MMI cavity with a 20 cm long MM fiber (solid curve).

shifts as the length of the MM fiber changes [14–16], an efficient fiber laser with diffraction-limited emissions is achievable by precisely controlling the length of the active MM fiber to overlap the transmission peak with the gain peak of the active ions as illustrated in Fig. 1.

The presence of mode conversion, which may result from core inhomogeneities, geometrical imperfection, microbending, strain, and pressure, is detrimental to the efficient and stable operation of an MMI fiber laser. The random mode conversion is increased with the MM fiber length [5]. Therefore, a short fiber cavity is preferred because the shorter the fiber cavity, the less random mode conversion will occur. A phosphate fiber laser can generate watt-level [21] or even ten-watt-level emission within a few centimeters doped fiber [22] owing to high solubility of rare-earth ions and low ion clustering effects in phosphate glass. Therefore, a heavily Er/Yb codoped MM phosphate fiber is well-suited to realize an MMI fiber laser.

The design of our MMI fiber laser is schematically shown in Fig. 2. A 10.236 cm long active MM phosphate fiber with a cladding of 125 μm is spliced to a 1 m long section of SMF-28. The MM core is codoped with 1 wt. % Er_2O_3 and 8 wt. % Yb_2O_3, respectively. The core diameter is 25 μm and the numerical aperture of the fiber is 0.17, which correspond to a normalized frequency $V=8.7$. Propagation of approximately 30 modes (including two polarizations each) is supported in this MM active fiber. The active fiber segment and an additional ~10 cm of SMF-28 are held in a straight silicon U-groove that is cooled by a water chiller. Most of the SMF-28 fiber segment is not stripped so that any cladding modes that might be excited by the modes of the MM fiber are effectively absorbed by the outer coating and diffraction-limited output is ensured.

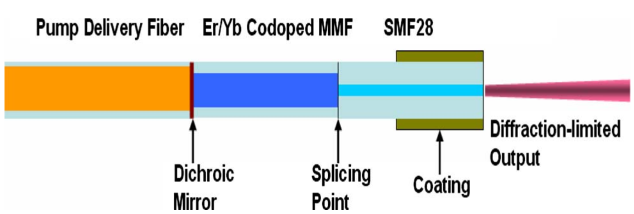

Fig. 2. (Color online) Design of the MMI fiber laser (the figure is not to scale).

The pump source is a 976 nm laser diode array coupled into an MM pump delivery fiber with a 105 μm core diameter, 125 μm outer diameter, and numerical aperture of 0.22. A dichroic coating, which has high reflectivity (>99.8%) at the laser wavelength (1535 nm) and high transmission (>92%) at the pump wavelength (975 nm), is deposited on the fiber end-facet. The pump delivery fiber is butt-coupled to the MM active fiber. Note that the length of the MM phosphate fiber section is precisely controlled to an accuracy of better than 10 μm. For a 10 cm long 25 μm MM fiber, a length deviation of 10 μm results in a transmission maximum shift of ~0.1 nm. A transmission peak ~1535.5 nm is obtained for the test hybrid cavity with a 10.236 cm long active MM fiber that overlaps well with the maximum gain of the active fiber.

The output power of this MMI fiber laser as a function of launched pump power is shown in Fig. 3 as squares and compared to the signal powers of a free-running MM fiber laser without an SMF-28 section (triangles). Both lasers have an active MM fiber section of ~10 cm. The MMI fiber laser reaches a maximum output power of more than 1 W that is limited by the available pump power. The slope efficiency is ~8.1%, which is very close to 9.2%, the efficiency of its free-running counterpart MM fiber laser without an SM section. A part of this difference might be attributed to imperfect splicing between the phosphate fiber and the silica fiber that results in some coupling losses. The single-transverse-mode output was confirmed by measuring the field distribution and a perfect fundamental mode with M^2 of 1.01 was observed. In contrast, M^2 of a free-running MM fiber laser was measured to be 2.5 at a low pump level and ~3.5 at higher pump levels.

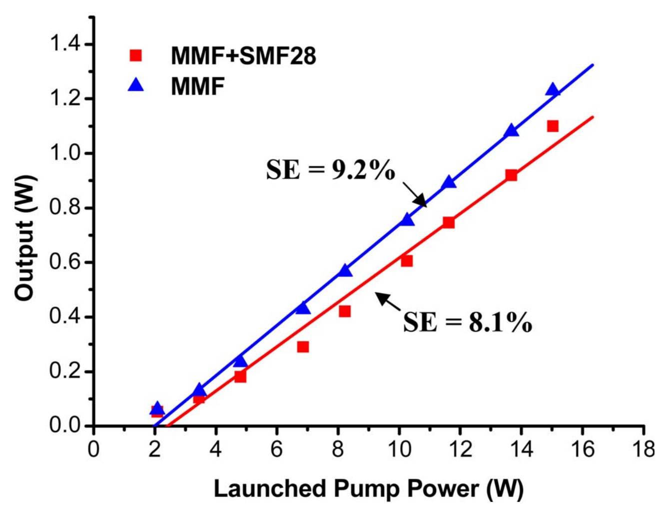

Fig. 3. (Color online) Output power as a function of launched pump power for an MMI fiber laser as shown in Fig. 2 (squares) and a free-running MM fiber laser (triangles).

The spectrum of a free-running MM fiber laser and that of the MMI laser at different pump levels are plotted in Fig. 4. In contrast to the broadband and multiwavelength operation of the free-running MM fiber laser, we observe only a single MMI laser emission peak with a 3 dB bandwidth clearly below 0.5 nm. Small bandwidth, single-peak emission indicates the spectral filtering effect of MMI during an in-phase operation [15] and the implications of the particular gain profile of a heavily Er/Yb codoped phosphate fiber as shown in Fig. 1. It is also observed that the emission peak moves toward shorter wavelengths and the bandwidth slightly broadens with an increase in pump power. The blueshift of the laser peak should result from the increased MM fiber length owing to thermal expansion at high pump levels. Some spectral broadening may be caused by a larger number of oscillating longitudinal laser modes.

It is worth noting here that, in all previous schemes of mode discrimination in fiber lasers with MM sections [3–9], only the fundamental mode of the MM section oscillates in the fiber laser cavity. In our MMI fiber laser, however, several transverse modes oscillate in the MM fiber section and constructively interfere at the splice point between the SM and MM fiber sections where they are transformed into the fundamental mode of the SMF. Therefore, the active mode volume of our MMI fiber laser is significantly increased compared to any fundamental-mode selection technique. In the test MMI fiber laser, three modes (LP_{01}, LP_{02}, and LP_{03}) were excited in the 25 μm MM section. Since most of the energy is stored at modes LP_{01} (64.4%) and LP_{02} (31.3%), the interference is simple and such an MMI fiber laser is very easy to construct. As the core size of the MM fiber becomes larger, more modes are excited and the interference will be more complicated [13,15]; however, self-imaging can still occur at certain MM fiber lengths and, therefore, MMI fiber lasers utilizing larger MM core sizes are feasible and will be the subject of future investigations.

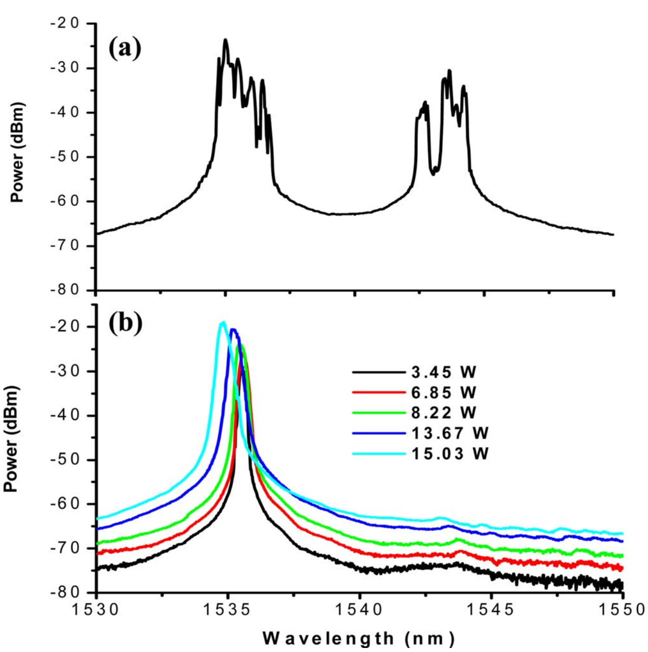

Fig. 4. (Color online) Emission spectra of (a) free-running MM and (b) MMI fiber lasers at various pump power levels.

In conclusion, we have demonstrated a new approach to achieve single-transverse-mode output from an active MM fiber by utilizing the self-imaging principle of MMI effects. Efficient and stable diffraction-limited emission with narrow bandwidth from an MMI fiber laser has been shown.

This work was supported by the National Science Foundation through grant 0725479 and the Arizona Technology and Research Initiative Fund.

References

1. X. Zhu and R. Jain, Opt. Lett. **32**, 26 (2007).
2. A. Schülzgen, L. Li, V. L. Temyanko, S. Suzuki, J. V. Moloney, and N. Peyhambarian, Opt. Express **14**, 7087 (2006).
3. H. L. Offerhaus, N. G. Broderick, D. J. Richardson, R. Sammut, J. Caplen, and L. Dong, Opt. Lett. **23**, 1683 (1998).
4. J. M. Sousa and O. G. Okhotnikov, Appl. Phys. Lett. **74**, 1528 (1999).
5. U. Griebner, R. Koch, H. Schonnagel, and R. Grunwald, Opt. Lett. **21**, 266 (1996).
6. A. Polynkin, P. Polynkin, A. Schülzgen, M. Mansuripur, and N. Peyghambarian, Opt. Lett. **30**, 403 (2005).
7. J. P. Koplow, D. A. V. Kliner, and L. Goldbergy, Opt. Lett. **25**, 442 (2000).
8. P. Wang, L. J. Cooper, J. K. Sahu, and W. A. Clarkson, Opt. Lett. **31**, 226 (2006).
9. L. Dong, J. Li, and X. Peng, Opt. Express **14**, 11512 (2006).
10. S. H. Baek and W. B. Roh, Opt. Lett. **29**, 153 (2004).
11. A. Mocofanescu, X. Zhu, L. Wang, and R. Jain, in *Conference on Lasers and Electro-Optics* (Optical Society of America, 2005), paper CMCC6.
12. L. B. Soldano and E. C. M. Penning, J. Lightwave Technol. **13**, 615 (1995).
13. A. J. Poustie, N. Finlayson, and P. Harper, Opt. Lett. **19**, 716 (1994).
14. R. Selvas, I. Torres-Gomez, A. Martinez-Rios, J. A. Alvarez-Chavez, D. A. May-Arrioja, P. Likamwa, A. Mehta, and E. G. Johnson, Opt. Express **13**, 9439 (2005).
15. W. S. Mohammed, P. W. E. Smith, and X. Gu, Opt. Lett. **31**, 2547 (2006).
16. W. S. Mohammed, A. Mehta, and E. G. Johnson, J. Lightwave Technol. **22**, 469 (2004).
17. Q. Wang and G. Farrell, Opt. Lett. **31**, 317 (2006).
18. A. Mehta, W. Mohammed, and E. G. Johnson, IEEE Photon. Technol. Lett. **15**, 1129 (2003).
19. Q. Li, C. Lin, P. Tseng, and H. P. Lee, Opt. Commun. **250**, 280 (2005).
20. H. Li, M. Brio, L. Li, A. Schülzgen, N. Peyghambarian, and J. V. Moloney, J. Opt. Soc. Am. B **24**, 2707 (2007).
21. L. Li, M. Morrell, T. Qiu, V. L. Temyanko, A. Schülzgen, A. Mafi, D. Kouznetsov, J. V. Moloney, T. Luo, S. Jiang, and N. Peyghambarian, Appl. Phys. Lett. **85**, 2721 (2004).
22. T. Qiu, L. Li, A. Schülzgen, V. L. Temyanko, T. Luo, S. Jiang, A. Mafi, J. V. Moloney, and N. Peyghambarian, IEEE Photon. Technol. Lett. **16**, 2592 (2004).